

Displacive phase transition in SrTiO₃ thin films grown on Si(001)

F. S. Aguirre-Tostado, A. Herrera-Gómez, J. C. Woicik, R. Droopad, Z. Yu, D. G. Schlom, J. Karapetrova, P. Zschack, and P. Pianetta

Citation: *Journal of Vacuum Science & Technology A* **22**, 1356 (2004); doi: 10.1116/1.1765657

View online: <http://dx.doi.org/10.1116/1.1765657>

View Table of Contents: <http://scitation.aip.org/content/avs/journal/jvsta/22/4?ver=pdfcov>

Published by the AVS: Science & Technology of Materials, Interfaces, and Processing

Articles you may be interested in

Phase transitions and domain stabilities in biaxially strained (001) SrTiO₃ epitaxial thin films

J. Appl. Phys. **108**, 084113 (2010); 10.1063/1.3488636

Directionally dependent ferroelectric phase transition order of anisotropic epitaxial Ba_xSr_{1-x}TiO₃ thin films

Appl. Phys. Lett. **88**, 012902 (2006); 10.1063/1.2161937

Dielectric characterization in a broad frequency and temperature range of SrBi₂Nb₂O₉ thin films grown on Pt electrodes

J. Appl. Phys. **97**, 114102 (2005); 10.1063/1.1904726

Pyroelectric response of ferroelectric thin films

J. Appl. Phys. **95**, 3618 (2004); 10.1063/1.1649460

Phase transitions in (Ba_{0.7}Sr_{0.3})TiO₃/(001) MgO thin film studied by Raman scattering

J. Appl. Phys. **93**, 9930 (2003); 10.1063/1.1574173

ADVERTISEMENT

Instruments for advanced science



Gas Analysis

- dynamic measurement of reaction gas streams
- catalysis and thermal analysis
- molecular beam studies
- dissolved species probes
- fermentation, environmental and ecological studies



Surface Science

- UHV TPD
- SIMS
- end point detection in ion beam etch
- elemental imaging - surface mapping



Plasma Diagnostics

- plasma source characterization
- etch and deposition process reaction kinetic studies
- analysis of neutral and radical species



Vacuum Analysis

- partial pressure measurement and control of process gases
- reactive sputter process control
- vacuum diagnostics
- vacuum coating process monitoring

contact Hiden Analytical for further details



info@hideninc.com
www.HidenAnalytical.com
 CLICK to view our product catalogue 

Displacive phase transition in SrTiO₃ thin films grown on Si(001)

F. S. Aguirre-Tostado^{a)} and A. Herrera-Gómez
CINVESTAV-Querétaro, Apartado Postal 1-798, Querétaro 76001, México

J. C. Woicik
National Institute of Standards and Technology, Gaithersburg, Maryland 20899

R. Droopad and Z. Yu
Physical Sciences Research Labs, Motorola, 2100 East Elliot Road, Tempe, Arizona 85284

D. G. Schlom
Materials Science and Engineering, Pennsylvania State University, University Park, Pennsylvania 16802

J. Karapetrova and P. Zschack
University of Illinois, APS-UNICAT, Argonne National Lab, Argonne, Illinois 60439

P. Pianetta
Stanford Synchrotron Radiation Laboratory, Stanford, California 94309

(Received 3 December 2003; accepted 5 May 2004; published 20 July 2004)

Polarization dependent near and extended x-ray absorption fine-structure (XANES and EXAFS), in combination with x-ray diffraction, has been used to study the structure of SrTiO₃ (STO) ultra thin films grown on Si(001). For the in-plane direction (200), the x-ray diffraction data indicate that all films (from 40 to 200 Å) are equally expanded. This is in contradiction to previous reports claiming that the growth is pseudomorphic and epitaxial (coherent), which would predict an inplane contraction. Even the thinnest films (40 Å) grow in a relaxed mode (not coherent) at the deposition temperature (700 °C). As the system is brought to room temperature, the films (now anchored to the substrate) are not allowed to compress as much as bulk STO. The residual film expansion is quantitatively explained by the differential thermal expansion of Si and STO. For the out-of-plane direction (002), the x-ray diffraction data indicate that STO films are expanded for the thinnest films, and relaxed for a thickness of 200 Å. The in-plane and out-of-plane EXAFS and XANES data show that the perpendicular expansion of the thinner films is accompanied by a displacive phase transition of SrTiO₃ where the Ti atom moves toward the (002) direction. This ferroelectric-type behavior of the thinner films implies important potential applications in electronics. © 2004 American Vacuum Society. [DOI: 10.1116/1.1765657]

I. INTRODUCTION

Strontium titanate (SrTiO₃ or STO) is a multifunctional material with a stable structure upon an extensive range of temperatures. STO is commonly used as substrate for the growth of various oxides with attractive electrical properties as for superconductors and ferroelectrics.¹ STO (STO) also works as a buffer layer for the growth III–V semiconductors on silicon allowing for the optical capabilities of III–V's with the robustness of Si technology.² The interest of STO as high-*k* gate dielectric to substitute SiO₂ is falling down due to large amount of problems that remains regarding the growth of a commensurate and sharp interface of STO with Si. However, the scientific and technologic importance of STO still remains.

At room temperature, bulk SrTiO₃ has a perovskite structure and can be described by placing Sr⁺² atoms at the corners of a cube, a Ti⁺⁴ atom at the cube center, and O⁻² atoms at the centers of the cube faces, in perfect octahedral coordination with the Ti⁺⁴ atom [Fig. 1(a)]. The phase transformations of bulk STO as a function of temperature has been studied in detail and is, at some extent, well understood.

At 105 K STO exhibits a phase transition where the oxygen octahedra rotates with a small tetragonal distortion of its unit cell ($c/a - 1 < 0.0001$).^{3,4} At 35 K, Curie law for the electrical permittivity predicts a ferroelectric phase transition.^{5,6} However, due to quantum fluctuations, any ferroelectricity is suppressed for all temperatures down to 0 K.⁷ Strontium titanate becomes ferroelectric under strain at very low temperatures.⁸ Physical properties of thin film are different from those of bulk materials. Moreover, mechanical properties of strained films could also differ from those films that are relaxed.⁹

Recently, the driving force of the semiconductor industry to integrate thin ferroelectric transition-metal oxides with Si transistor technology has revived the question of whether or not a ferroelectric ground state can be supported by an ultrathin film.¹⁰ Recent experimental studies designed to address this issue have focused on ferroelectric materials that were grown in a two-dimensional, thin-film geometry.^{11,12} In this work we present x-ray diffraction (XRD) evidence that the growth of STO thin films on silicon is not coherent, rather, the films remains under residual tensile strain at room temperature. The films also exhibit an elastic anomaly where the volume of STO unit cell increases, giving rise to a negative

^{a)}Electronic mail: saguirre@fis.cinvestav.mx

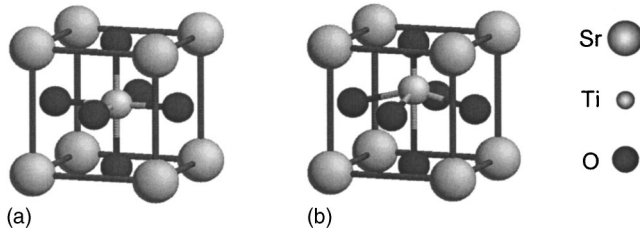


FIG. 1. STO unit cell. (a) Cubic and (b) tetragonal.

Poisson ratio. This anomaly is accompanied by a displacive phase transition of the Ti atom in the (002) direction, as demonstrated by the x-ray absorption fine structure (XAFS) measurements. The functionality of this ferroelectric instability as gate dielectric in metal-oxide-semiconductor field-effect transistor (MOSFET's) devices for nonvolatile memories is still under study.

II. EXPERIMENTS

STO films with thicknesses of 40, 60, 80, and 200 Å were grown on Si(001) substrates using molecular beam epitaxy. Details of the sample preparation are provided elsewhere.¹³ Near and extended x-ray absorption fine-structure (XANES and EXAFS) data were collected for the Ti *K* edge ($h\nu = 4966$ eV) at room temperature. The data were recorded by monitoring the Ti *K_α* fluorescence emission using a single-element SiLi detector fixed in the horizontal plane, at a right angle to the incident photon beam. The absorption data were collected in two orientations, with the polarization vector *e* of the synchrotron radiation aligned either parallel (*e* in-plane) or perpendicular (*e* out-of-plane) to the Si(001) surface. Consequently, due to the two-dimensional nature of the surface/film/substrate geometry, it was possible to distinguish in-plane from out-of-plane Ti–O bonding. In addition, the x-ray absorption spectrum from finely ground STO powder was measured in transmission; it was used as the EXAFS phase and amplitude standard to *experimentally* determine the Ti–O bond lengths within the films.

In order to characterize the strain state of the STO films, high-resolution specular x-ray diffraction measurements using a crystal analyzer were performed around the STO(002) and Si(200) Bragg reflections. Figure 2 shows the results of the diffraction experiment for the perpendicular lattice constants of the STO films. Clearly, the effect of strain is evident for samples thinner than a critical thickness of ~ 80 Å (the horizontal line denotes the bulk lattice constant of STO).

III. RESULTS AND DISCUSSIONS

Due to the extremely large lattice mismatch between the cubic unit cells of STO and Si ($a_{\text{STO}} = 3.905$ Å and $a_{\text{Si}} = 5.431$ Å), epitaxial growth of a thin STO layer on a Si(001) substrate results in a STO layer that is rotated around the Si[001] surface-normal by 45°; i.e., STO[100]//Si[110]. The resulting lattice mismatch between the STO layer and Si(001) is then equal to $(a_{\text{Si}}/\sqrt{2} - a_{\text{STO}})/a_{\text{STO}} = -1.7\%$.¹³ In a coherent growth, a thin enough film is expected to be in

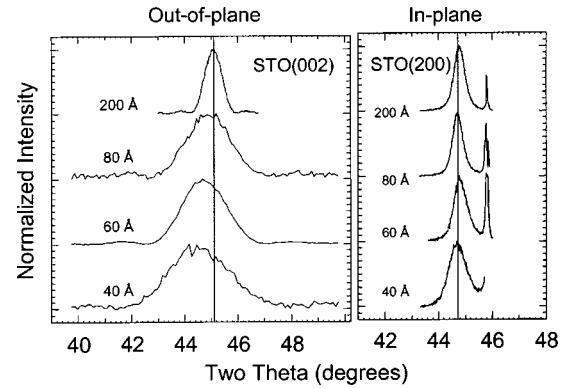


FIG. 2. Out-of-plane (right) and in-plane (left) by x-ray diffraction data of the 40, 60, 80, and 200 Å STO films.

perfect registry with the substrate. An isotropic cubic layer contracted in the in-plane direction will be Poisson expanded in the out of plane direction according to the following relation:

$$\epsilon_{\perp} = -2(c_{12}/c_{11})\epsilon_{\parallel}, \quad (1)$$

where c_{11} and c_{12} are the elastic constants, $\epsilon_{\parallel} = 1 - a_{\parallel}/a_{\text{bulk}}$ and $\epsilon_{\perp} = 1 - a_{\perp}/a_{\text{bulk}}$ are the in-plane and out-of-plane strains, respectively. a_{\parallel} , a_{\perp} , and a_{bulk} are the in-plane, out-of-plane and bulk lattice constants, respectively. Both a_{\parallel} and a_{\perp} , for STO films (for thicknesses of 40, 60, 80, and 200 Å), were obtained from the XRD curves showed in Fig. 2. These values are plotted in Fig. 3, where the squares are the values for the in-plane lattice constants and the circles are those of the out-of-plane direction. Using the macroscopic elastic constants of STO (Ref. 14) and the translation of the out-of-plane strain to the in-plane strain as stated by Eq. (1), the behavior of a_{\perp} is in accordance to an epitaxial growth, where the in-plane lattice constant is very similar to that of the substrate. However, when we look at the in-plane XRD to determine a_{\parallel} , we found that all the films are expanded, this result is totally opposite of what is expected for a pseudomorphic growth. Regardless of the thicknesses (in the range

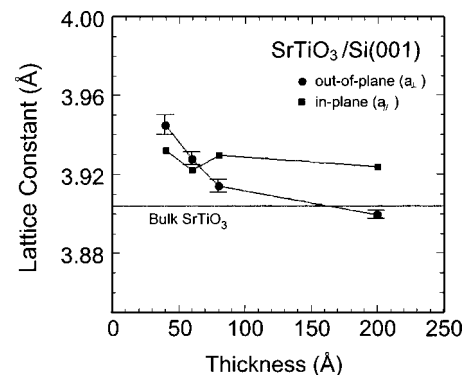


FIG. 3. Out-of-plane (circles) and in-plane (squares) lattice constants of the 40, 60, 80, and 200 Å STO films as determined by x-ray diffraction. The dotted line shows the bulk cubic lattice constant of STO.

of 40–200 Å) and within the experimental error bars, all the STO films grown on Si(001) are under tensile strain with a value of residual strain of ~2%.

As showed in Fig. 3 for the 80 Å and below, the STO films are expanded in both direction. This volume increase in the unit cell is a severe elastic anomaly revealed by a negative Poisson ratio. The residual tensile strain in the in-plane direction is due to the differential thermal expansion between the STO film and the silicon substrate, while the expansion in the out-of-plane direction is the effect of a polarized interfacial layer of STO as evidenced by the x-ray absorption fine structure measurements.

The coefficients of thermal linear expansion are $\alpha_{\text{STO}} = 10.8 \times 10^{-6} \text{ K}^{-1}$ for SrTiO₃ (Ref. 15) and $\alpha_{\text{Si}} = 2.49 \times 10^{-6} \text{ K}^{-1}$ for Si.¹⁶ This significant difference causes the lattice mismatch to be larger at the growth temperature, where the expanded substrate and film lattice constant are 3.847 and 3.930 Å. If we suppose that the film relaxes at the growth temperature, even for the thinnest film, then when the whole structure (substrate+film) cools down to room temperature, the film will contract only the amount that the substrate contract. That means that the substrate will contract a 0.18% ($a_{\text{Si}}: 3.847 \text{ Å} \rightarrow 3.840 \text{ Å}$). If the film lattice constant contracts a 0.18% then the final lattice constant will be 3.923 Å. This is the thermal mechanism through the substrate+film system behaves giving rise to the formation of a residual tensile strain.

Figure 4 shows the Ti *K* x-ray absorption near-edge spectra from the thin films studied. The spectra have been scaled to equal edge jump. The pre-edge features occur in the region of 4965–4980 eV. As is well known, in pure octahedral (O_h) symmetry the transition-metal 3*d* states are split by the ligand-crystal field into a triply degenerate t_{2g} set and a doubly degenerate e_g set, with a splitting of ~2 eV, as indicated in Fig. 4. In molecular point groups that lack inversion symmetry, for example the tetrahedral (T_d) point group, the metal 4*p* orbitals mix with the metal 3*d* orbitals, but this mixing occurs only with the higher of the two crystal-field split 3*d* states.¹⁷ This *p-d* mixing makes 1*s* transitions to the higher energy group of 3*d* states dipole allowed (1*s*→3*d* transitions are dipole forbidden).¹⁸ For this reason, the intensity of the second pre-edge feature has been correlated with ferroelectricity in the perovskite structure,^{19,20} i.e., with the quantitative displacement of the central Ti cation from its centrosymmetric position within the perovskite unit cell. Our data show a large increase in intensity of the Ti *K* pre-edge feature with decreasing film thickness. These data suggest the existence of an interfacial ferroelectric layer that becomes less significant as the film grows. The difference in the pre-edge height among the in- and out-of-plane polarizations (see Fig. 4) reveals the existence of a preferential axis along which the Ti atoms are displaced. Most of the growth of the pre-edge height in the in-plane direction is due to a disordered layer close to the interface with the Si(001) substrate where the formation of SiO₂ plays an important role. However, major evidence of the displacement of the Ti atom

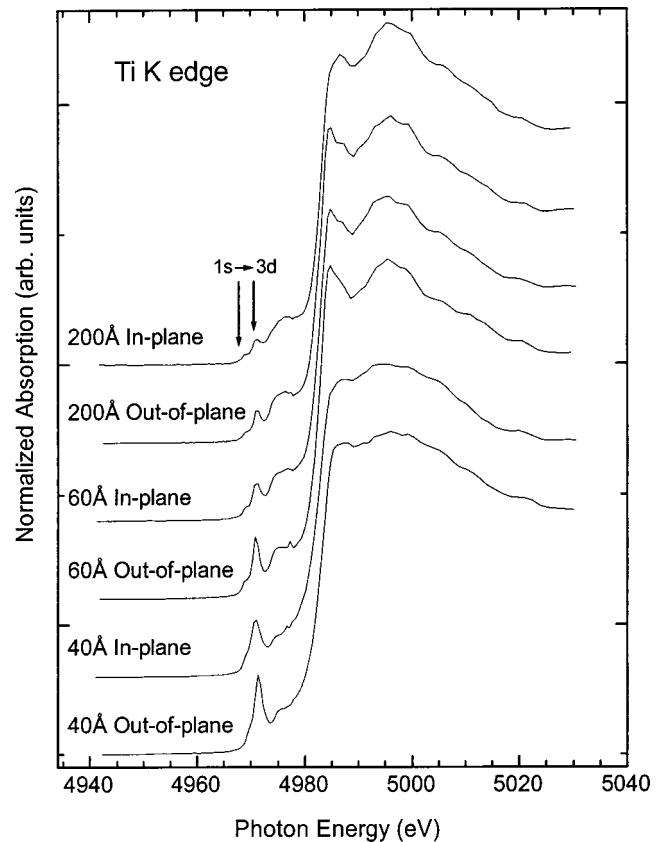


FIG. 4. Ti *K* near-edge x-ray absorption spectra from thin STO films recorded with the polarization vector in-plane and out-of-plane (see the text). The data have been normalized to equal edge jump. The energy positions of the 1*s*→3*d* transitions are indicated. The data have been offset for clarity.

from its centrosymmetric position is obtained from the quantitative EXAFS analysis.

We turn now to our extended x-ray absorption fine-structure data. Little difference between the 200 Å film and the powder is observed for either of the two film polarizations; however, the situation is much different for the thinner films that show both significant polarization and thickness effects. Figure 5 shows the Fourier transforms of the extended fine structure. The peak in the Fourier transform near 1.4 Å corresponds to the Ti–O bond length.²¹ Most startling is an apparent splitting of the Ti–O bond length for the thinner films when the polarization vector is aligned perpendicular to the STO/Si interface.

To obtain quantitative results, the Ti–O radial shell was modeled with the EXAFS phase and amplitude functions obtained from the bulk STO powder. As anticipated, data recorded from the 200 Å film in either polarization were indistinguishable from the STO powder. The results of the modeling for the 60 Å film are shown in Fig. 6. (Results for the 40 Å film are similar, but with larger errors.) The top panel shows the fit to the data from the 60 Å film recorded with the polarization vector in-plane, and the middle panel shows the fit to the data from the 60 Å film recorded with the polarization vector out-of-plane, both assuming a single Ti–O bond length. Clearly, a beat occurs in the out-of-plane

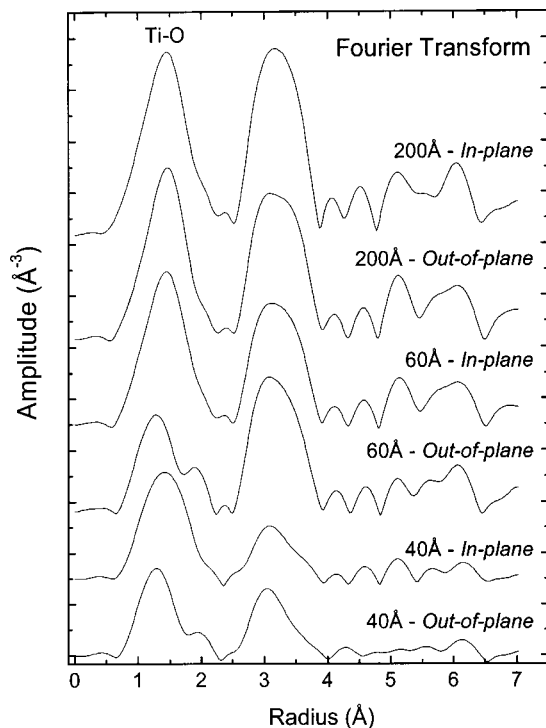


FIG. 5. Fourier transforms of the EXAFS data from the thin STO films recorded with the polarization vector in-plane and out-of-plane (see the text). The data have been offset for clarity.

data near $k=7 \text{ \AA}^{-1}$ that is not modeled by a single Ti–O distance. Our two-shell analysis (bottom panel) finds the Ti–O bond length to be split by $0.22 \pm 0.06 \text{ \AA}$ along the Si[001] surface-normal direction. Within the error bars, the bond lengths obtained by EXAFS (see Fig. 6) are in agreement with the lattice constant measured by XRD. The amount of the Ti–O bond length splitting does not depend on the STO film thickness but is stronger for thinner films. This

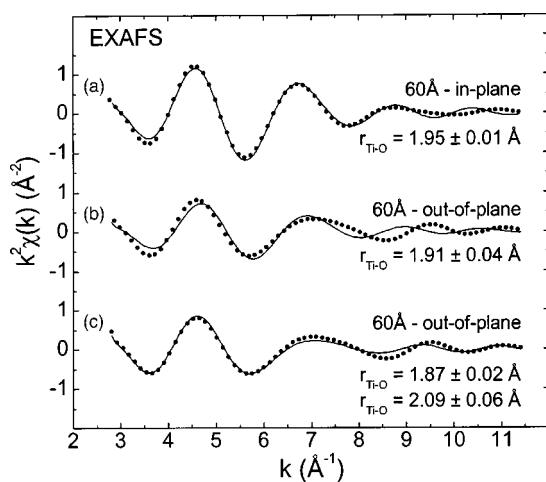


FIG. 6. Fits to the Fourier-filtered, first-shell contributions to the k^2 -weighted Ti K -edge EXAFS from the 60 Å film using the phase and amplitude functions obtained from the STO powder. The dots are the data points of the backtransform, and the solid lines are the fits. (a) In-plane data using one Ti–O distance. (b) Out-of-plane data using one Ti–O distance. (c) Out-of-plane data using two Ti–O distances.

result confirms the formation of an interfacial polarized layer of STO. This work is an experimental evidence of the correlation existing between ferroelectricity in STO and the increase in the unit cell volume predicted by Ref. 22.

IV. CONCLUSIONS

The differential thermal expansion coefficients of SrTiO₃ and Si combined with the elastic constants of SrTiO₃ indicate that the films disorder at growth temperature. The SrTiO₃ films are then under tensile (not compressive) strain at room temperature. In contradiction to previous reports claiming that the growth of SrTiO₃ on Si(001) is coherent.²³ X-ray diffraction data therefore witnesses a severe elastic anomaly; i.e., a negative Poisson ratio, in the thinnest films. X-ray absorption fine-structure (Ti K edge) finds a local Ti–O bond-length distortion that is interpreted as a ferroelectric polarization [see Fig. 1(b)]. The observed ferroelectric phase transition in STO is accompanied by an increment in the unit cell volume which is uncommon in ferroelectric phases of other perovskites where the unit cell volume is nearly conserved. This polarization is apparent for the thinnest films, but decreases with film thickness. SrTiO₃ thin film growth on Si is not coherent, rather, the films are under residual tensile strain due to differential thermal expansion. These films exhibit an elastic anomaly; that is explained by the presence of an interfacial polarization as revealed by x-ray absorption fine structure.

ACKNOWLEDGMENTS

Research carried out (in whole or in part) at the National Synchrotron Light Source, Brookhaven National Laboratory, which is supported by the U.S. Department of Energy, Division of Materials Sciences and Division of Chemical Sciences, under Contract No. DE-AC02-98CH10886. The UNICAT facility at the Advanced Photon Source (APS) is supported by the University of Illinois at Urbana-Champaign, Materials Research Laboratory (U.S. DOE, the State of Illinois-IBHE-HECA, and the NSF), the Oak Ridge National Laboratory (U.S. DOE under contract with UT-Battelle LLC), the National Institute of Standards and Technology (U.S. Department of Commerce), and UOP LLC. The APS is supported by the U.S. DOE, Basic Energy Sciences, Office of Science under contract No. W-31-109-ENG-38. Additional support was provided by the Consejo Nacional de Ciencia y Tecnología of México (CONACyT Projects 34721-E, 33901-U, G33178-U) and the Stanford Linear Accelerator Center (CRADA—Project No. 158). The authors would like to thank to M.A. Hernández-Landaverde for technical support.

¹M. Kawasaki, K. Takahashi, T. Maeda, R. Tsuchiya, M. Shinohara, O. Ishiyama, T. Yonezawa, M. Yoshimoto, and H. Koinuma, *Science* **266**(5190), 1540 (1994).

²K. Eisenbeiser, R. Emrick, R. Droopad, Z. Yu, J. Finder, S. Rockwell, J. Holmes, C. Overgaard, and W. Ooms, *IEEE Electron Device Lett.* **23**, 300 (2002).

³K. A. Müller, W. Berlinger, and F. Waldner, *Phys. Rev. Lett.* **21**, 814 (1968).

⁴G. Shirane and Y. Yamada, *Phys. Rev.* **177**, 858 (1969).

- ⁵H. P. R. Frederikse, W. R. Thurber, and W. R. Hosler, *Phys. Rev.* **134**, A442 (1964).
- ⁶M. Fisher, A. Lahmar, M. Maglione, A. San Miguel, J. P. Itié, A. Polain, and F. Baudelet, *Phys. Rev. B* **49**, 12451 (1994).
- ⁷W. Zhong and David Vanderbilt, *Phys. Rev. B* **53**, 5047 (1996).
- ⁸H. Uwe and T. Sakudo, *Phys. Rev. B* **13**, 271 (1976).
- ⁹A. A. Sirenko, I. A. Akimov, J. R. Fox, A. M. Clark, Hong-Cheng Li, Weidong Si, and X. X. Xi, *Phys. Rev. Lett.* **82**, 4500 (1999).
- ¹⁰J. Junquera and P. Ghosez, *Nature (London)* **422**, 506 (2003).
- ¹¹A. V. Bune, V. M. Fridkin, S. Ducharme, L. M. Blinov, S. P. Palto, A. V. Sorokin, S. G. Yudin, and A. Zlatkin, *Nature (London)* **391**, 874 (1998).
- ¹²T. Tybell, C. H. Ahn, and J.-M. Triscone, *Appl. Phys. Lett.* **75**, 856 (1999).
- ¹³Z. Yu, J. Ramdani, J. A. Curless, J. M. Finder, C. D. Overgaard, R. Droopad, K. W. Eisenbeiser, J. A. Hallmark, and W. J. Ooms, *J. Vac. Sci. Technol. B* **18**, 1653 (2000).
- ¹⁴R. O. Bell and G. Rupprecht, *Phys. Rev.* **129**, 90 (1963).
- ¹⁵D. de Ligny and P. Richet, *Phys. Rev. B* **53**, 3013 (1996).
- ¹⁶D. R. Lide, *CRC Handbook of Chemistry and Physics*, 80th ed. (CRC, Boca Raton, FL, 2000), pp. 12–97.
- ¹⁷F. A. Cotton, *Chemical Applications of Group Theory* (Wiley, New York, 1971), Chap. 8.
- ¹⁸J. Wong, F. W. Lytle, R. P. Messmer, and D. H. Maylotte, *Phys. Rev. B* **30**, 5596 (1984).
- ¹⁹R. V. Vedrinskii, V. L. Kraizman, A. A. Novakovich, Ph. V. Demekhin, and S. V. Urazhdin, *J. Phys.: Condens. Matter* **10**, 9561 (1998).
- ²⁰B. Ravel, E. A. Stern, R. I. Vedrinskii, and V. Kraizman, *Ferroelectrics* **206–207**, 407 (1998).
- ²¹D. E. Sayers, E. A. Stern, and F. W. Lytle, *Phys. Rev. Lett.* **27**, 1204 (1971).
- ²²N. Sai and D. Vanderbilt, *Phys. Rev. B* **62**, 13942 (2000).
- ²³R. A. McKee, F. J. Walker, and M. F. Chisholm, *Phys. Rev. Lett.* **81**, 3014 (1998).